



Fracture-hosted fluid-rock reactions within geothermal reservoirs of the eastern Trans-Mexican Volcanic Belt

Alicja Lacinska^{1*}, Chris Rochelle¹, Andrew Kilpatrick¹, Jeremy Rushton¹, Leandra M. Weydt², Kristian Bär² and Ingo Sass^{2,3}

¹British Geological Survey, Nicker Hill, Keyworth, Nottingham, NG12 5GG, UK

²Department of Geothermal Science and Technology, Technische Universität Darmstadt, Schnittpahnstraße 9, 64287 Darmstadt, Germany

³Darmstadt Graduate School of Excellence Energy Science and Engineering, Otto-Berndt-Straße 3, 64287 Darmstadt, Germany

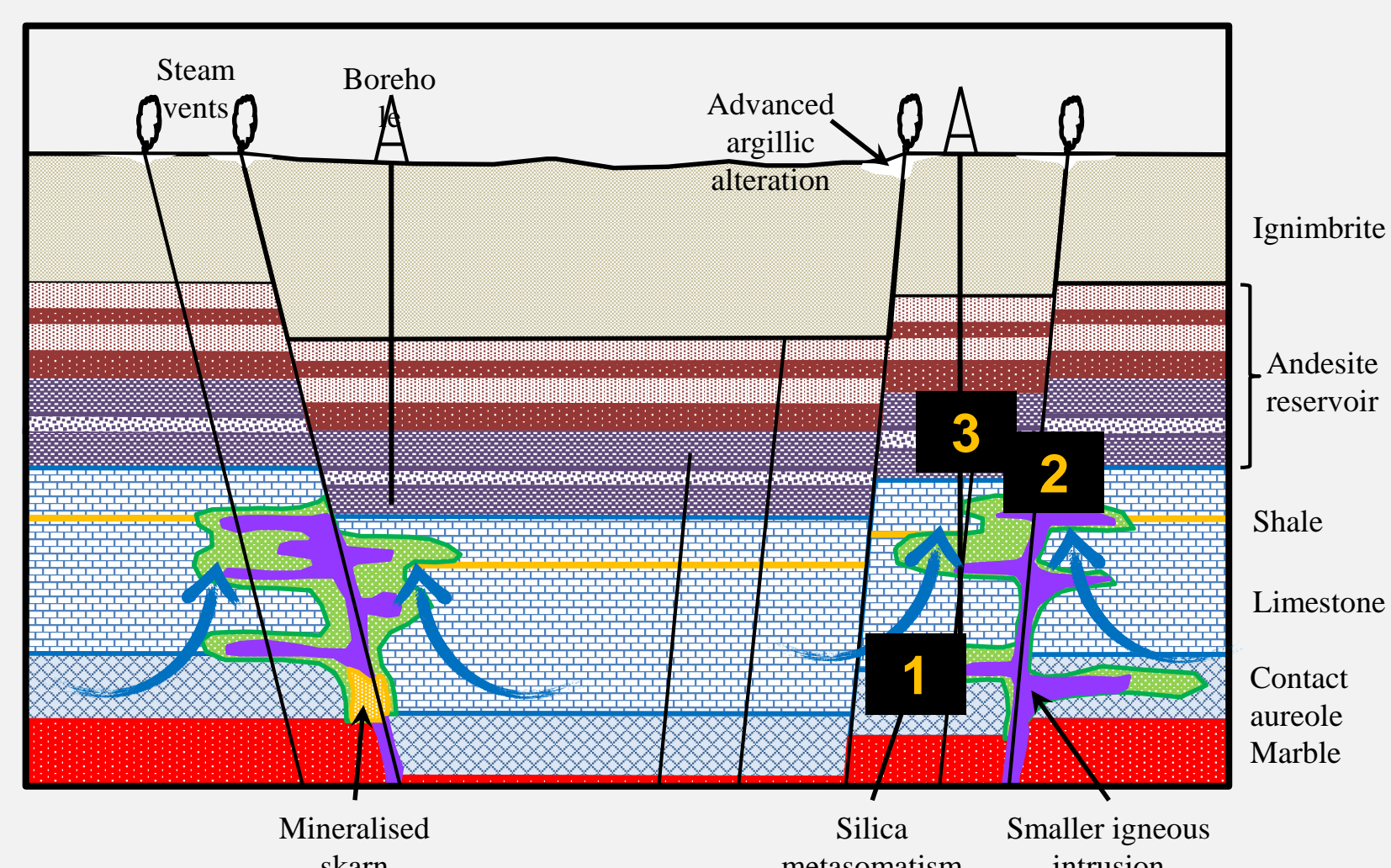
Introduction

Fractures within hydrothermal systems represent major flow pathways facilitating the onset of natural convection¹ and subsequent maintenance of fluid flow.

It is vital to understand processes occurring along such fractures as these will impact the productivity of hot fluids during geothermal exploitation.

This is especially important where fluid movement crosses contrasting rock types, resulting in a range of fluid-rock reactions, mineral dissolution and precipitation, and changes in fracture permeability.

Fig 1. Schematic of hydrothermal flow within a geothermal system. Numbers 1-3 correspond to the examples of fluid-rock reactions presented on this poster.



Methods

Scanning electron microscopy was performed using:

- FEI Quanta 600 SEM with an Oxford Instruments X-Max detector (SDD) for Energy Dispersive Spectrometry (EDS), running with Oxford Instruments INCA (v4) software. SEM operating at 20 kV accelerating voltage, approximately 5 nA beam current; and an acquisition time of 60 seconds per spot was used. EDS process time of 4 resulted in dead-times of <45%.
- Zeiss SIGMA 300VP Mineralogic system over selected areas for large scale PHASE MAPS, at least 5 x 5 mm in size, up to and including full section areas (23 x 36 mm). SEM operating at 20 kV, with the 120 µm aperture and 'beam boost' on to give a nominal beam current of 20 nA. Mapping was performed with a beam step size of ~10 to 5 µm and a dwell time of 10 ms. Phase identifications were based on normalised quantitative EDX data passed through expert-user-defined filters. Outputs were formed by combining data from multiple adjacent fields of view, mosaicked into phase map images with associated BSE images.

Summary

An understanding of the interplay between mineral chemistry, rates of fluid-rock reaction and texture of a metasomatic assemblage within/and adjacent to fractures is essential to create viable models for the potential temporal evolution of fracture flow/sealing.

The petrographic study provided a compelling evidence for:

- The presence of dolomitic marbles in the area studied
- Silica metasomatism, $\pm \text{H}_2\text{O}$, $\pm \text{Fe}$, $\pm \text{Al}$, $\pm \text{Mg}$, $\pm \text{Cr}$, $\pm \text{V}$, ($\pm \text{K}$), resulting in the formation of anhydrous (forsterite, diopside, spinel) and hydrous Mg silicates (talc, tremolite, phlogopite). *Implications: presence of talc in fractures and metasomatic veins might result in zones of weakness and slip*
- Late stage hydrothermal event responsible for hydration of originally unhydrous phases, e.g. forsterite-serpentine
- Mineral transformation-related volume change. The increase or decrease of the volume of solid phases results in significant micro-fracturing. *Implications: enhanced permeability for initial CO_2 escape and subsequent ingress of later H_2O -rich fluids, variable degree of lithological coherency-incoherency. Alteration of diopside along fractures by late hydrothermal fluids resulting in the formation of talc (low frictional strength).*
- Differential stress during brucite marble formation. *Implications: variable properties of the rock when measured in different direction*

Fluid – rock reactions

1 High T metasomatism in brucite marble

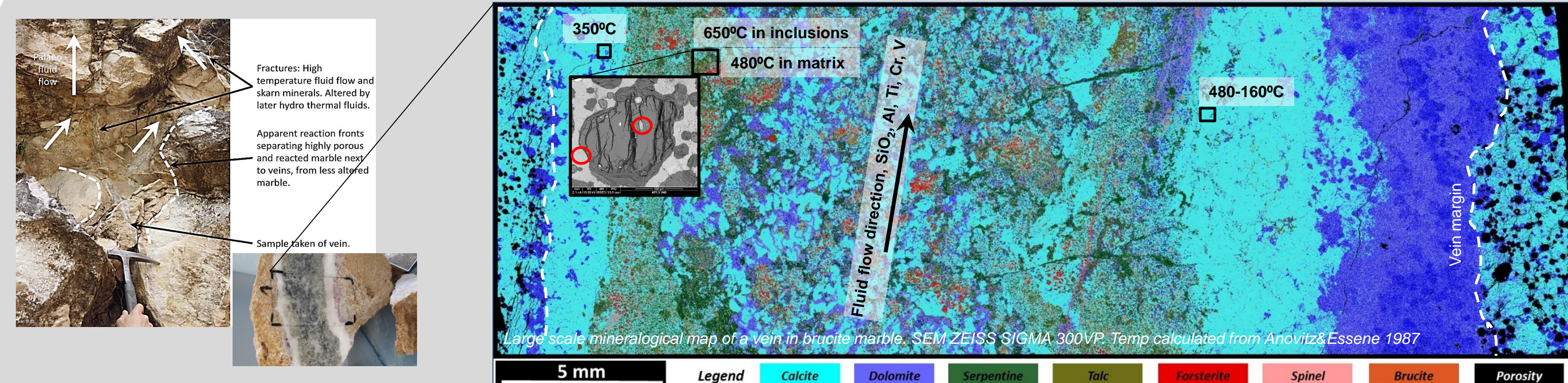


Fig 2. BSE images of A – brucite marble and B – partially serpentinised forsterite spinel skarn in the vein

Prograde reactions

Thermal metamorphism and formation of periclase marble
 $\text{CaMg}(\text{CO}_3)_2 \rightarrow \text{CaCO}_3 + \text{MgO} + \text{CO}_2$ (ΔV approximately -25%)

Hydration of periclase to brucite
 $\text{MgO} + \text{H}_2\text{O} \rightarrow \text{Mg}(\text{OH})_2$ (ΔV approximately +45%)

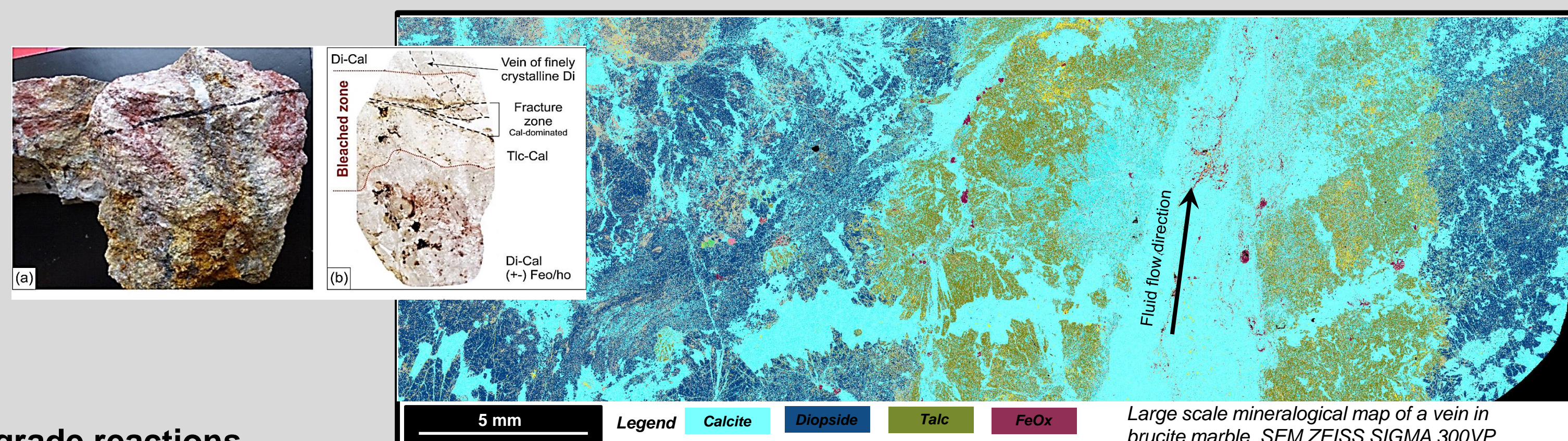
Formation of forsterite
 $2\text{MgO} + \text{SiO}_2 \Rightarrow \text{Mg}_2\text{SiO}_4$

Formation of spinel
 $\text{MgO} + \text{Al}_2\text{O}_3 \Rightarrow \text{MgAl}_2\text{O}_4$

Retrograde reactions

Formation of serpentine minerals
 $2\text{Mg}_2\text{SiO}_4 + 3\text{H}_2\text{O} \Rightarrow \text{Mg}_3\text{Si}_2\text{O}_5(\text{OH})_4 + \text{Mg}(\text{OH})_2$
(ΔV approximately +30%)

2 High T metasomatism in limestone overprinted with hydrothermal alteration



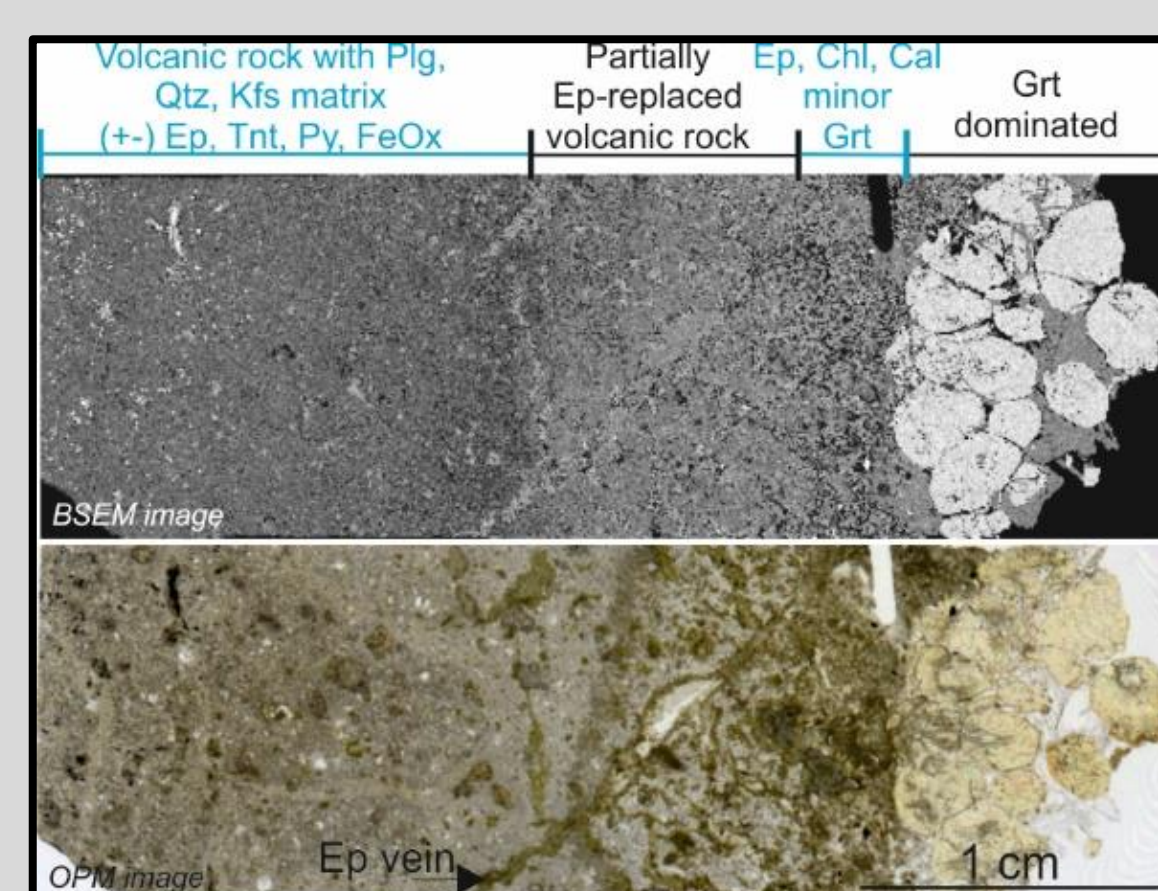
Prograde reactions

Formation of diopside
 $2\text{CaCO}_3 + 2\text{SiO}_{2(\text{aq})} + \text{Mg}^{2+} \Rightarrow \text{CaMgSi}_2\text{O}_6 + \text{Ca}^{2+} + 2\text{CO}_2$ (ΔV approximately -10%)

Retrograde reactions

Formation of talc
 $3\text{CaMgSi}_2\text{O}_6 + 6\text{H}^+ \Rightarrow \text{Mg}_3\text{Si}_4\text{O}_{10}(\text{OH})_2 + 2\text{SiO}_2 + 3\text{Ca}^{2+} + 2\text{H}_2\text{O}$

3 Metasomatic reaction in andesite



Formation of epidote
 $3\text{CaAl}_2\text{Si}_2\text{O}_8 + \text{Ca}^{2+} + 2\text{H}_2\text{O} \Rightarrow 2\text{Ca}_2\text{Al}_3\text{Si}_3\text{O}_{12}(\text{OH}) + 2\text{H}^+$

Formation of andradite
 $\text{CaAl}_2\text{Si}_2\text{O}_8 + 5\text{Ca}^{2+} + 2\text{Fe}^{3+} + 4\text{SiO}_2 + 8\text{H}_2\text{O} \Rightarrow 2\text{Ca}_3[\text{Fe,Al}]_2\text{Si}_3\text{O}_{12} + 16\text{H}^+$

Mineralogical changes with the distance from fracture:

- Fracture to 0.5 cm: Epidote + calcite + chlorite + garnet, with volcanic textures largely overprinted by the alteration: dissolution-related secondary porosity and epidotisation
- 0.5 to 1.5 cm: Dominantly epidote-replaced volcanic rock with subordinate titanite and amphibole. Numerous ≤ 2 mm wide epidote and calcite + epidote (+ minor chlorite) veins
- 1.5 cm onwards: Locally bleached and altered volcanic rock. The alteration encompasses localised formation of epidote and chlorite, both partially replacing the rock matrix and the scattered phenocrysts of amphibole and plagioclase.



This project has received funding from the European Union's Horizon 2020 research and innovation programme under grant agreement No. 727550 and the Mexican Energy Sustainability Fund CONACYT-SENER, project 2015-04-68074



Partners



CFE

We acknowledge the Comision Federal de Electricidad (CFE) for kindly providing support and advice and for granting access to their geothermal fields. Data has been kindly provided by CFE. We also acknowledge our Mexican colleagues for their help and collaboration.

The content of this presentation reflects only the authors' view. The Innovation and Networks Executive Agency (INEA) is not responsible for any use that may be made of the information it contains.

Contact us

Alicja M Lacinska alci@bgs.ac.uk
Christopher Rochelle caro@bgs.ac.uk

Visit us
www.gemex-h2020.eu

